SAR reduced excitation by joint design of RF pulse and slice selective gradient shape

Christoph Stefan Aigner[1], Christian Clason[2], Armin Rund[3], and Rudolf Stollberger[1]

[1]*Institute of Medical Engineering, Graz University of Technology, Graz, Austria,* [2]*Faculty of Mathematics, University of Duisburg-Essen, Essen, Germany,* [3]*Institute for Mathematics and Scientific Computing, University of Graz, Graz, Austria*

INTRODUCTION: The application of MRI at high field strengths is still limited by the specific absorption rate (SAR). To reduce the energy of a specific RF pulse, the VERSE principle[1] can be applied, which starts from a specific RF-shape and changes the pulse energy by adaption of the RF and gradient amplitude. In a simulation study, this idea was generalized and reformulated as an optimal control problem (gVERSE[2]). However, the numerical solution was based on applying commercial software to a formulation as a standard discrete nonlinear optimization problem, which limited the approach to a coarse spatial resolution of the slice profile and lead to a strong dependence on the specific software used.[2] In this work, we present a joint design of a SAR reduced RF pulse with a time dependent slice selective gradient using exact derivatives calculated by the adjoint approach[3]. This approach allows computing optimal pulses and gradients for high-resolution slice profiles. Simulation results are validated by phantom measurements and in vivo applications.

THEORY: The optimal control approach consists in computing the RF pulse $B_{1,y}(t)$ and the slice selective gradient $G_z(t)$ that minimize the mean squared error (MSE) after refocusing between the numerical solution $M(T;\, z)$ and a prescribed slice profile $M_d(z)$ together with a quadratic cost term modeling the SAR of the pulse:

$$\mathrm{J(M,B)} = \frac{1}{2}\int_{z_{\min}}^{z_{\max}} |\mathrm{M(T;z)} - \mathrm{M_d(z)}|_2^2 \,\mathrm{dz} + \frac{\alpha}{2}\int_0^{\mathrm{T}} |B_{1,y}(t)|^2 \,\mathrm{dt} + \frac{\beta}{2}\int_0^{\mathrm{T}} |G_z(t)|^2 \,\mathrm{dt}.$$

The magnetization vector $M(T;\, z)$ is the solution of the full time-dependent Bloch equation in the rotating frame $\dot{\mathrm{M}} = \mathrm{B}\times\mathrm{M} + \mathrm{R(M)}$ (R being the relaxation term and $\mathrm{B(t,z)} = (B_{1,x}(t)\,, B_{1,y}(t)\,, \mathrm{G_z(t)\cdot z})$ with the control variables $B_{1,y}(t)$ and $G_z(t)$; $B_{1,x}(t)$ is set to zero. The parameters α and β control the trade-off between the competing goals of slice profile attainment and SAR reduction. The optimization is done using a globally convergent trust-region Newton method[4] with a matrix-free iterative solution of the Newton step using the adjoint calculus. To achieve accurate derivative information, we discretize the Bloch equation such that the discretized derivatives coincide with the derivatives of the discretized functional (adjoint-consistency).

METHODS: The desired magnetization M_d consists of three components (x,y,z) for every spatial point and is set to a gauss-filtered rectangular slice with a thickness of 5mm and a flip angle of 90° after refocusing at the time T = 3.48ms. The excitation pulse has a duration of 2.56ms with 256 samples (dt = 10µs) and is followed by a refocusing pulse (zero RF pulse, standard trapezoidal gradient with 50% area; not part of the optimization). The spatial resolution is set to be 0.2mm with 2001 samples to incorporate a distance of ±0.2m. The starting point for the optimization is a constant zero pulse and a constant gradient of -10mT/m. To achieve a good balance between the slice profile accuracy and a SAR reduction we choose α = 0.25e-3 and β = 0.1e-3; in the case of an RF only optimization, β is set to zero and the Gz gradient is held constant at -10 mT/m. The optimized shapes were imported to a GRE sequence and implemented on a 3T MR scanner (Magnetom Skyra, Siemens Healthcare, Erlangen, Germany) to verify the simulations by phantom and an in vivo experiment of a volunteer.

RESULTS AND DISCUSSION: Figure 1 compares the optimization results of the RF pulse with a prescribed slice selective gradient (A) and the joint design (B) of both vectors. It can be seen that $B_{1,y}(t)$ and $G_z(t)$ are tightly connected and in areas of high RF amplitude, e.g. at the center of the pulse, the shape gets stretched and the gradient amplitude is lowered by almost 40% which reduces the RF power significantly (by 30%; see also Table 1) while keeping the MSE comparably low (0.26% vs. 0.31%). The peak slew rate of the optimized gradient (120mT/mms) remains well below the maximal rate (180mT/mms) of the used scanner system. The measured slice profiles shown in Figure 3 verify the numerical simulation of Figure 2 and show a steep transition between the in- and out-of-slice regions as well as a homogeneous flip angle distribution across the slice. In Figure 4 we compare two reconstructed transverse images of an in vivo experiment. Using the same imaging parameters as in the phantom experiment it can be seen that the overall image quality does not change even though the RF power is reduced.

CONCLUSION: The presented approach allows for an efficient design of low-SAR RF pulses for a given slice profile. The proposed method is based on the full Bloch equations and is therefore able to incorporate large flip angles and relaxation. Furthermore, a matrix-free approach allows incorporating exact derivative information in a highly efficient manner, leading to a high resolution of the optimized slice profile (e.g. 2001 spatial points). The results demonstrate the applicability and the ability to reduce the power of the RF pulse while creating an accurate slice profile. Depending on the regularization parameters and α and β, it is possible to compute pulses with an even lower SAR. However, hardware limitations, in particular the gradient slew rate, can restrict practical implementation. The simultaneous optimization of RF pulse and gradient shape can also be applied to other problems such as minimal phase or simultaneous multislice excitation.

REFERENCES: 1. Conolly S., et al. JMR 1988; 78:440-458. 2. Anand CK., et al. Algorithmic Operations Research 2011; 6:1-19. 3. Aigner CS., et al. ISMRM 22 (2014). p. 1448. 4. Steihaug SINUM 1983; 20:626-637.

ACKNOWLEDGEMENT: supported by FWF "SFB F3209-18"

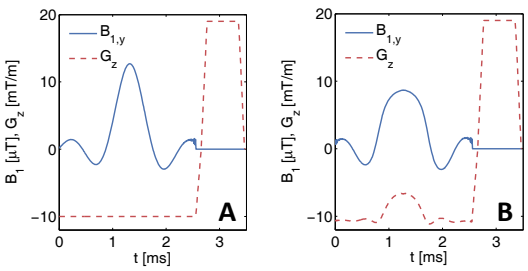

Figure 1: RF only (A) and joint RF/Gz (B) optimization

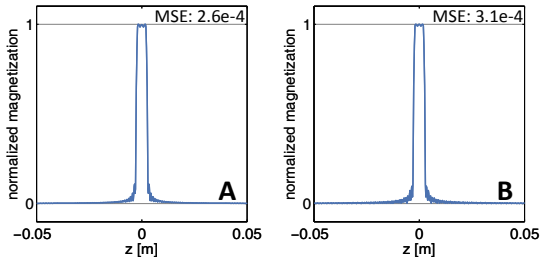

Figure 2: Simulated transverse magnetization

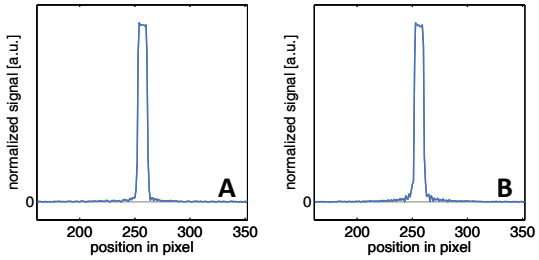

Figure 3: Measured magnetization

Table 1: Comparison on B1 power and B1 peak

	A	B
$\|\boldsymbol{B_{1,y}}\|_2^2$ [a.u.]	73.5	52.6
$\|\boldsymbol{B_{1,y}}\|_\infty$ [µT]	13.4	8.7

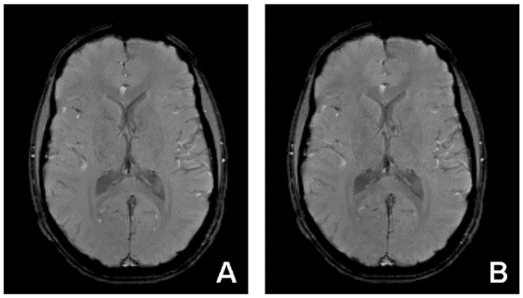

Figure 4: Comparison of in vivo reconstruction using the RF pulse and gradient shape shown in Figure 1